U.S. Department of
Transportation

**Federal Railroad
Administration**

Broken Rim Detection Using Proximity Sensors

Office of Research,
Development
and Technology
Washington, DC 20590

DOT/FRA/ORD-20/45

Final Report
November 2020

REPORT DOCUMENTATION PAGE

Form Approved
OMB No. 0704-0188

Public reporting burden for this collection of information is estimated to average 1 hour per response, including the time for reviewing instructions, searching existing data sources, gathering and maintaining the data needed, and completing and reviewing the collection of information. Send comments regarding this burden estimate or any other aspect of this collection of information, including suggestions for reducing this burden, to Washington Headquarters Services, Directorate for Information Operations and Reports, 1215 Jefferson Davis Highway, Suite 1204, Arlington, VA 22202-4302, and to the Office of Management and Budget, Paperwork Reduction Project (0704-0188), Washington, DC 20503.

1. AGENCY USE ONLY (Leave blank)	2. REPORT DATE November 2020	3. REPORT TYPE AND DATES COVERED Technical Report February–April 2014

4. TITLE AND SUBTITLE Broken Rim Detection Using Proximity Sensors	5. FUNDING NUMBERS DTFR53-11-D-00008
6. AUTHOR(S) Matthew Witte and Juan Gallardo	Task Order 328

7. PERFORMING ORGANIZATION NAME(S) AND ADDRESS(ES) Transportation Technology Center, Inc. 55500 DOT Road Pueblo, CO 81001	8. PERFORMING ORGANIZATION REPORT NUMBER

9. SPONSORING/MONITORING AGENCY NAME(S) AND ADDRESS(ES) U.S. Department of Transportation Federal Railroad Administration Office of Railroad Policy and Development Office of Research, Development and Technology Washington, DC 20590	10. SPONSORING/MONITORING AGENCY REPORT NUMBER DOT/FRA/ORD-20/45

11. SUPPLEMENTARY NOTES
COR: Monique Ferguson Stewart

12a. DISTRIBUTION/AVAILABILITY STATEMENT This document is available to the public through the FRA website.	12b. DISTRIBUTION CODE

13. ABSTRACT (Maximum 200 words)
Transportation Technology Center, Inc. (TTCI) performed research and testing on a broken rim detector concept by Diesel Intellect International (DII). The detector uses proximity sensors to detect the presence of rim material overhanging the field side of the rail. The concept was tested with both ultrasonic and magnetic sensors. Initial feasibility was carried out using ultrasonic sensors, but it was unsuitable for the railroad environment. The device with magnetic sensors did not reliably detect a 0.75-inch deep by 4-inch long gouge on the corner of the wheel rim. The wheel position influenced by hunting and tread wear causes greater deviation in the signal than the calibration notch. The device configuration using magnetic sensors is unsuitable for broken rim detection.

14. SUBJECT TERMS Broken rim detector, ultrasonic sensors, magnetic sensors, High Tonnage Loop, HTL, wheel, track, rolling stock, testing, research, detector	15. NUMBER OF PAGES 28
	16. PRICE CODE

17. SECURITY CLASSIFICATION OF REPORT Unclassified	18. SECURITY CLASSIFICATION OF THIS PAGE Unclassified	19. SECURITY CLASSIFICATION OF ABSTRACT Unclassified	20. LIMITATION OF ABSTRACT

NSN 7540-01-280-5500

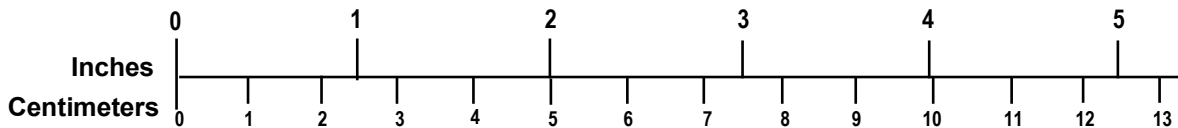Standard Form 298 (Rev. 2-89)
Prescribed by
ANSI Std. 239-18
298-102
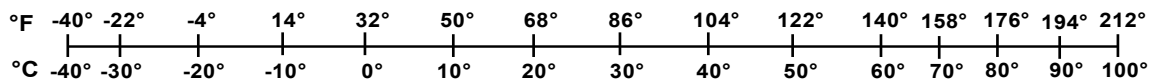
METRIC/ENGLISH CONVERSION FACTORS

ENGLISH TO METRIC

LENGTH (APPROXIMATE)

1 inch (in)	=	2.5 centimeters (cm)
1 foot (ft)	=	30 centimeters (cm)
1 yard (yd)	=	0.9 meter (m)
1 mile (mi)	=	1.6 kilometers (km)

AREA (APPROXIMATE)

1 square inch (sq in, in^2)	=	6.5 square centimeters (cm^2)
1 square foot (sq ft, ft^2)	=	0.09 square meter (m^2)
1 square yard (sq yd, yd^2)	=	0.8 square meter (m^2)
1 square mile (sq mi, mi^2)	=	2.6 square kilometers (km^2)
1 acre = 0.4 hectare (he)	=	4,000 square meters (m^2)

MASS - WEIGHT (APPROXIMATE)

1 ounce (oz)	=	28 grams (gm)
1 pound (lb)	=	0.45 kilogram (kg)
1 short ton = 2,000 pounds (lb)	=	0.9 tonne (t)

VOLUME (APPROXIMATE)

1 teaspoon (tsp)	=	5 milliliters (ml)
1 tablespoon (tbsp)	=	15 milliliters (ml)
1 fluid ounce (fl oz)	=	30 milliliters (ml)
1 cup (c)	=	0.24 liter (l)
1 pint (pt)	=	0.47 liter (l)
1 quart (qt)	=	0.96 liter (l)
1 gallon (gal)	=	3.8 liters (l)
1 cubic foot (cu ft, ft^3)	=	0.03 cubic meter (m^3)
1 cubic yard (cu yd, yd^3)	=	0.76 cubic meter (m^3)

TEMPERATURE (EXACT)

$[(x-32)(5/9)]$ °F = y °C

METRIC TO ENGLISH

LENGTH (APPROXIMATE)

1 millimeter (mm)	=	0.04 inch (in)
1 centimeter (cm)	=	0.4 inch (in)
1 meter (m)	=	3.3 feet (ft)
1 meter (m)	=	1.1 yards (yd)
1 kilometer (km)	=	0.6 mile (mi)

AREA (APPROXIMATE)

1 square centimeter (cm^2)	=	0.16 square inch (sq in, in^2)
1 square meter (m^2)	=	1.2 square yards (sq yd, yd^2)
1 square kilometer (km^2)	=	0.4 square mile (sq mi, mi^2)
10,000 square meters (m^2)	=	1 hectare (ha) = 2.5 acres

MASS - WEIGHT (APPROXIMATE)

1 gram (gm)	=	0.036 ounce (oz)
1 kilogram (kg)	=	2.2 pounds (lb)
1 tonne (t)	=	1,000 kilograms (kg)
	=	1.1 short tons

VOLUME (APPROXIMATE)

1 milliliter (ml)	=	0.03 fluid ounce (fl oz)
1 liter (l)	=	2.1 pints (pt)
1 liter (l)	=	1.06 quarts (qt)
1 liter (l)	=	0.26 gallon (gal)
1 cubic meter (m^3)	=	36 cubic feet (cu ft, ft^3)
1 cubic meter (m^3)	=	1.3 cubic yards (cu yd, yd^3)

TEMPERATURE (EXACT)

$[(9/5) y + 32]$ °C = x °F

QUICK INCH - CENTIMETER LENGTH CONVERSION

	0	1	2	3	4	5

Inches

Centimeters 0 1 2 3 4 5 6 7 8 9 10 11 12 13

QUICK FAHRENHEIT - CELSIUS TEMPERATURE CONVERSIO

°F	-40°	-22°	-4°	14°	32°	50°	68°	86°	104°	122°	140°	158°	176°	194°	212°
°C	-40°	-30°	-20°	-10°	0°	10°	20°	30°	40°	50°	60°	70°	80°	90°	100°

For more exact and or other conversion factors, see NIST Miscellaneous Publication 286, Units of Weights and Measures. Price $2.50 SD Catalog No. C13 10286   **Updated 6/17/98**

ii

Contents

Illustrations

Tables

Executive Summary

From February to April 2014, the Federal Railroad Administration (FRA) and the Association of American Railroads (AAR) funded Transportation Technology Center, Inc. (TTCI) to determine that the broken rim detector system as designed is not sensitive enough to detect a 4-inch (10.2 cm) long by 0.75-inch (1.9 cm) deep gouge on the rim. A broken rim detector is a track mounted device for detecting broken railroad wheel rims on moving trains. The device relies on a direct measurement of material presence to determine rim integrity. If the rim is missing a substantial portion of material, the proximity sensor should sense this void and alert that the wheel is broken. Such a system does not sense internal defects.

Testing at the Transportation Technology Center (TTC) in Pueblo, CO, resulted in an understanding that the magnetic sensors are unable to differentiate this geometric aberration from wheel position variations due to hunting and tread wear. While the sensors are reliable at sensing the distance to ferromagnetic material, they are relatively insensitive to voids in the material. The sensors respond to the closest portion of the target. As such, the sensors will only react to the missing piece if the void is large enough to completely miss the magnetic field of the sensor. Any small portion of metal remaining within range will be detected as "good" material, thus rendering the detector insensitive to all but the largest defects.

1. Introduction

From February to April 2014, Transportation Technology Center, Inc. (TTCI) performed research on new and emerging automated cracked wheel detectors under joint sponsorship of the Association of American Railroads (AAR) and the Federal Railroad Administration (FRA). As part of this work, TTCI tested a concept called a broken rim detector from Diesel Intellect International (DII). The broken rim detector employs a series of proximity sensors to detect the presence of rim material overhanging the field side of the rail. It is intended to find broken rims where a chunk of material is already missing. It does not function to detect internal wheel defects. This report details the findings from the development of this system.

1.1 Background

The broken rim detector is a straightforward approach to broken wheel detection. It does not require any special trackwork and has no moving parts. It uses a direct physical measurement to detect defects, and operates at line speeds. The approach could function either as a stand-alone detector, especially for cold environments where broken rim failures can develop quickly, or as a pre-inspection for cracked wheel inspection systems that use a tread bearing track work. Detecting and diverting vertical split rim wheels before they enter a rim-edge bearing track segment would minimize the risk of wheel drop derailment.

1.2 Overall Approach

The broken rim detector is an alternative to ultrasonic inspection technology that directly identifies wheels that have missing rim material. It is based on the concept that proximity sensor output is proportional to the distance between the sensor and the target. Essentially, it uses proximity sensors to detect wheel rim presence. An array of proximity sensors is mounted just beyond the field side of the railhead. As a good wheel passes, it will trigger every sensor equally in succession. If a damaged wheel passes, the signal will be different on one or more of the sensors. Analysis of the signals is required to identify the rim defects. The result is direct detection of a discontinuity in the rim.

1.3 Organization of the Report

This report summarizes the research introduced and its findings in Section 1. Section 2 identifies the history of ultrasonic and magnetic sensors and their purpose. Section 3 details the system configuration of the sensors. Section 4 briefly discusses the installation of the broken rim detector hardware. Section 5 documents the placement of the broken rim detector and the testing involved, while Section 6 outlines the results. Section 7 offers a conclusion to the research performed.

2. History

2.1 Ultrasonic Sensors

TTCI and DII performed a proof of concept test on the broken rim detector technology in 2012. This prototype test was with a broken rim detector model that used ultrasonic proximity sensors. The early prototype sensed both rim and flange continuity. Figure 1 shows a photograph of the early ultrasonic sensor-based device.

Figure 1. Broken Rim Detector Proof of Concept Prototype with Ultrasonic Sensors

The ultrasonic sensors are directional proximity sensors that emit a pulse of ultrasonic energy and then time the return echo to determine the distance of the target from the sensor. The system consisted of 33 sensors spaced 3.5 inches (9 cm) apart. Each sensor inspected a 7.9-inch (20 cm) sector of the passing wheel. The prototype pictured has sensors for detecting both the flange and the rim. The rim sensors face inward toward face of the rim. Figure 2 shows a typical signal from the rim sensors on a good wheel. All 33 channels are displayed.
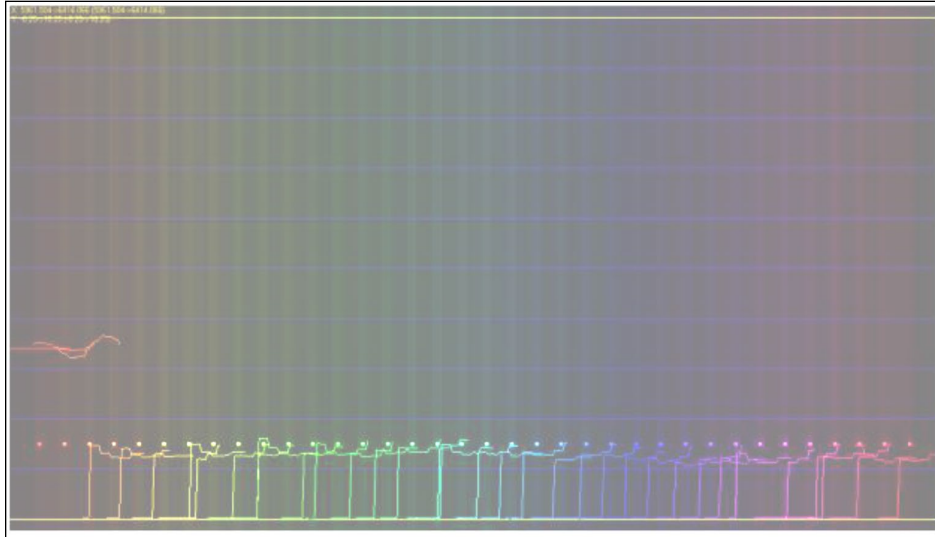
Figure 2. 33-Channel Ultrasonic Sensor Output for a Good Wheel Rim

Observe that the signals are uniform for a good wheel. The magnitude and duration of the signal from every sensor is the same.

Anomalies in the signal can arise from several sources. Lateral position of the wheel on the track (hunting) will change the magnitude of the signal, but changes from sensor to senor are gradual as the entire wheel is moving laterally. Hunting shows as a low frequency sinusoid across all the sensors. There are also sources of higher frequency noise. Figure 3 shows narrow spikes occurring at some of the sensors, which indicated small surface defects.
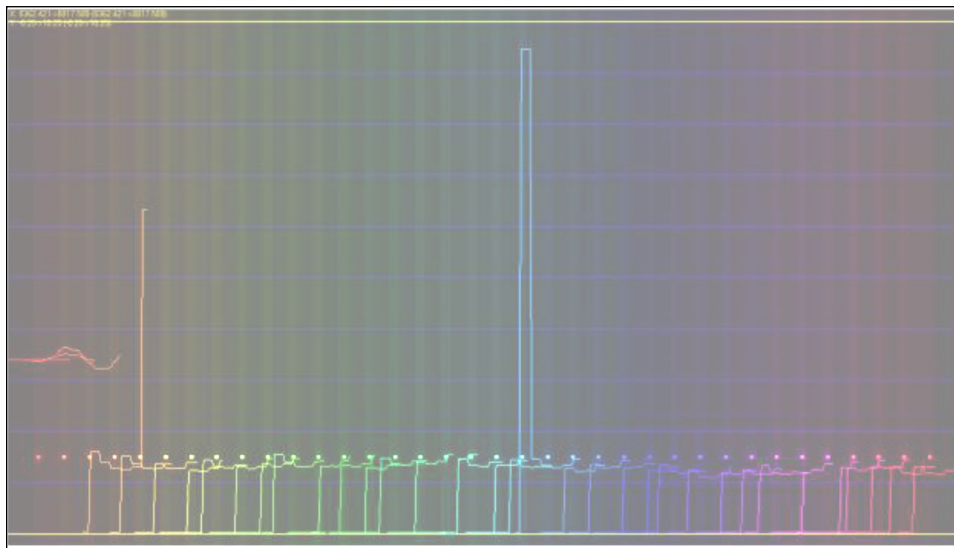
Figure 3. Narrow Spikes Occur at Small Surface Defects

These narrow spikes are likely the result of a missing reflection from small surface defects such as shelling or rolled edge. Figure 4 shows the test wheel associated with the signals in Figure 3.

Figure 4. Wheel With Rolled Rim That Created Narrow Spikes in the Ultrasonic Data

When a wheel with a shattered rim passes the system, the indication is much more pronounced. Figure 5 shows the result of a 35 mph pass of a shattered rim wheel. Figure 6 shows the wheel itself.

Figure 5. Ultrasonic Indication from a Shattered Rim

Figure 6. Shattered Rim that Caused the Indication in Figure 5

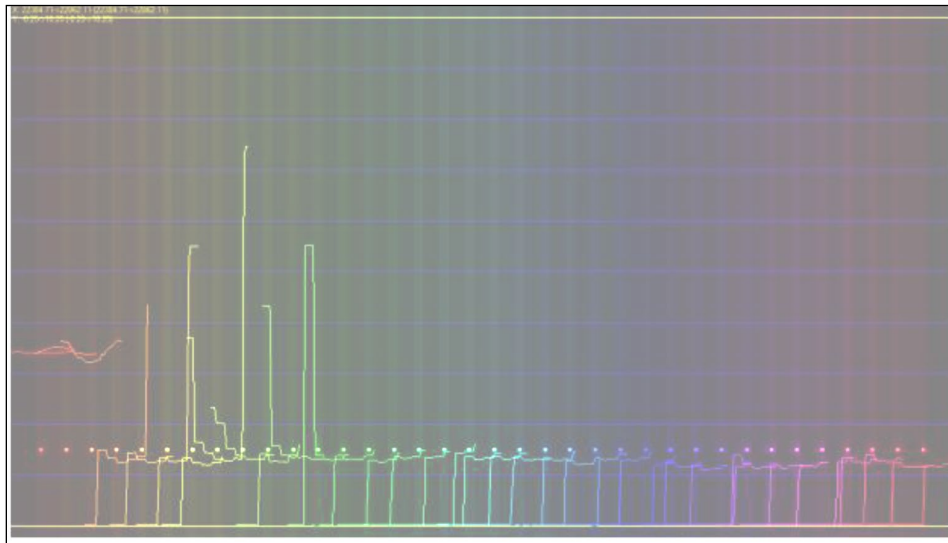The DII broken rim detector with ultrasonic probes identifies three criteria in the signal that signify a shattered rim. First is that a group of consecutive sensors has unusual readings. In this case, it is seven sensors. Next, the magnitudes of the signals are on the order of two times the nominal value. The sensors get the reflection earlier and from a greater distance than nominal. This is because the sensors "see" the void as it approaches on the rotating wheel, sensing the missing material while it is still some distance from the sensor.

Although this concept shows promise, the ultrasonic approach is not suitable for extended use in the railroad environment for several reasons. First, the configuration of sensors is unacceptable, while clearance is not adequate due to the ultrasonic sensors violating clearance requirements. Next, the ultrasonic sensors, bracketing, and cables are not suitable for the railroad environment. Finally, the ultrasonic sensors are sensitive to any airborne debris. Debris kicked up by the train causes noise in the signals. Any airborne material, rain, snow, dust, or even tumbleweeds cause noise that could be misconstrued as a defect. The system cannot function in poor weather conditions.

2.2 Magnetic Sensors

To be a commercially viable product, the technology requires a more robust sensor and a more compact design. Magnetic wheel sensors provide a robust and reliable alternative. Figure 7 shows a photo of a magnetic wheel sensor that DII used on other systems.

Figure 7. Magnetic Wheel Sensor

While reliability of the magnetic sensors is well established, they do operate differently than the ultrasonic probes. First, they are arranged to be facing upward just outboard of the field side of the railhead. They sense the portion of the rim overhanging the railhead. The wheel rim produces an electrical signal when it passes over the sensor surface. The signal amplitude is proportional to the wheel speed, mass, and distance to the sensor. Compared to the ultrasonic sensors, the magnetic sensors have the advantages of analog real-time output, which is not limited by speed and the sensors do not react to airborne dust and debris including rain and snow. They can operate in any weather condition.

However, the signal form from the sensors is different. Figure 8 shows a comparison of the typical signal from the ultrasonic sensor compared to the signal from the magnetic sensor.
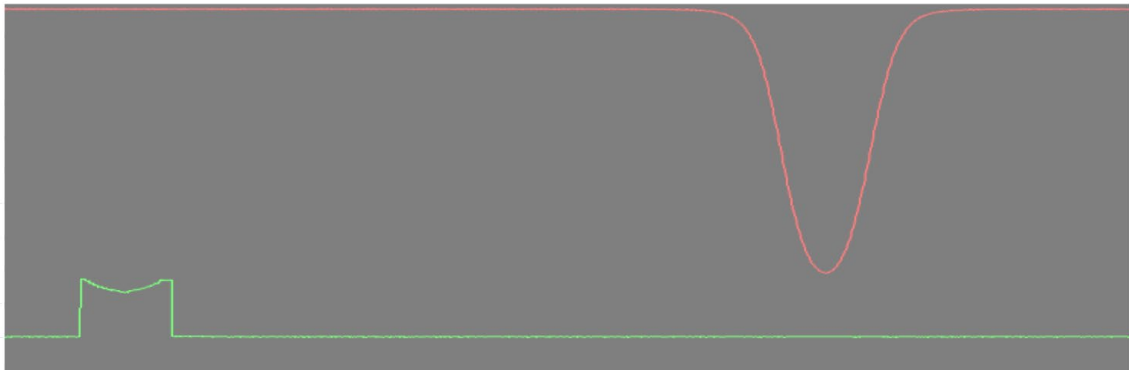

Figure 8. Comparison of Signals from the Ultrasonic Sensor (green) and Magnetic Sensors (red)

The signals between the sensor types are different, because the physical sensing is fundamentally different. The magnetic sensor detects ferromagnetic materials that distort its field. The signal it

produces is proportional to distance, size, and speed of the passing target. When placed up along the field side of the railhead, as shown in Figure 7, it will sense the portion of the wheel tread overhanging the railhead. If the wheel rim is closer to the sensor, the signal will be higher. A missing part of the rim will change the signal form. The following investigation explores the nature of this signal.

Specifications on the wheel sensor suggest that it has a 2-inch range and a resolution of less than 0.047 inches. DII surmised that this sensor would be acceptable for the broken rim detector application based on these specifications so a prototype was designed, built, and tested.

3. System Configuration

Each magnetic sensor covers 2 inches of the rim surface. An array of 64 sensors per rail is required to inspect a complete wheel circumference. The magnetic sensors are substantially wider than the ultrasonic sensors and they require a gap between them to prevent their fields from overlapping and causing cross talk. Because of this, they cannot be placed close enough together to sense the wheel in only one revolution. Therefore, their position must be staggered so that each sensor will sense a different segment of the rim over two revolutions. Figure 9 shows the concept of the sensor layout.
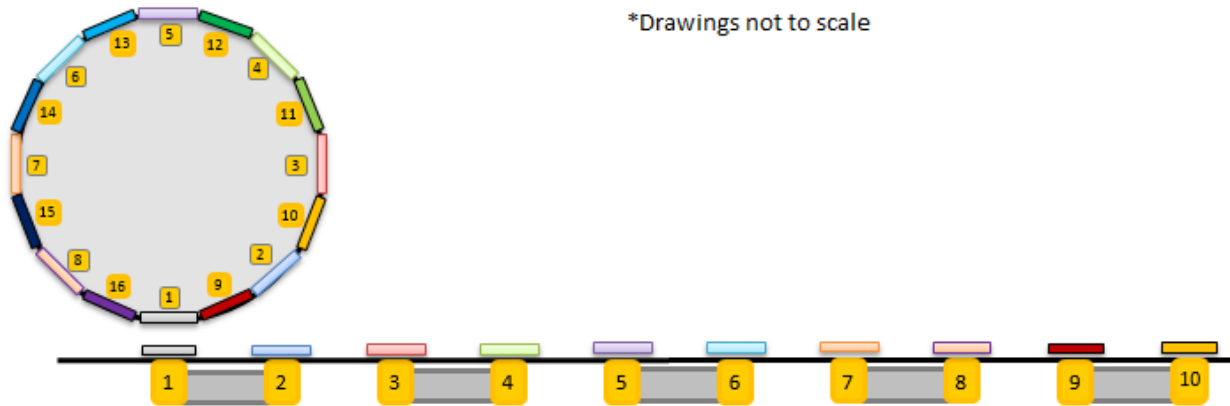

Figure 9. Staggered Sensor Spacing to inspect Entire Wheel over Two Revolutions

Sensors are mounted in pairs that must be precisely positioned and well aligned across the track. Lateral and vertical positioning will affect the magnitude of the signal, and longitudinal alignment across the track will affect the timing of the peak signal at each location. Each pair of sensors shares a bracket which mounts to the rail between the ties. The clamp is a commercially available piece of equipment that passes under the rail and attaches to the flange. Slotted brackets were designed to attach to the clamp. Brackets are slotted to accommodate uneven tie spacing. The range of adjustment must be sufficient to precisely stagger and align the sensors. Figure 10 shows a detail of the sensor mounting bracket assembly.

9
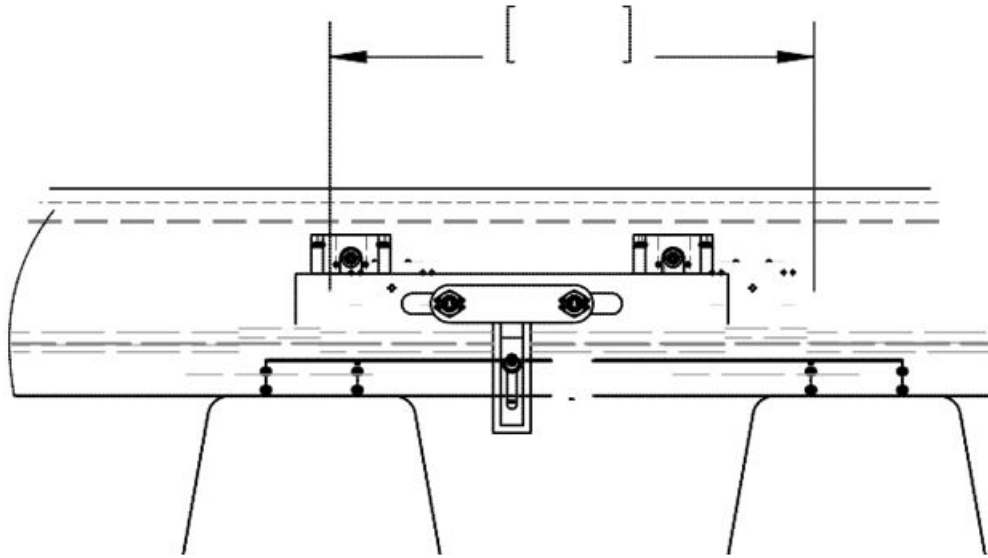
Figure 10. Sensor Mounting Clamp and Bracket Assembly

Figure 11 shows a perspective sketch of the magnetic sensors relative to the wheel.
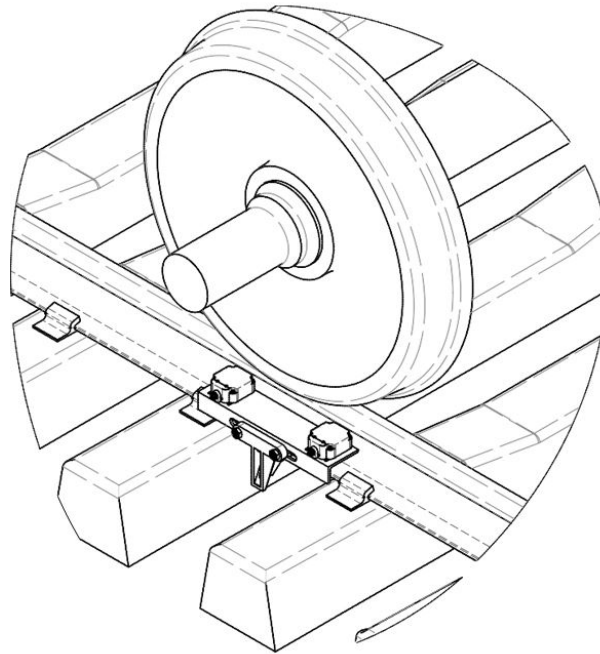
Figure 11**. Perspective View of the Sensors and Mounting Bracket Relative to the Wheel**

The rim of the wheel overhangs the rail and passes within the detection range of the sensors. The sensors precisely measure the distance to the rim. Figure 12 shows the worst-case clearance to the sensor for a worn wheel profile.

Figure 12. Clearance to Sensor with Worn Wheel Profile

The photo in Figure 12 shows the wheel in flange contact with the rail. This condition puts the rim of the worn wheel as close to the sensor as possible. A new wheel in the same position would be higher by approximately 0.50 inches.

Comparatively, the wheel on the other side for an axle in this position would be almost out of the range of the sensor. This wheel would produce a very low magnitude signal. This could happen if the axle is hunting. Hunting could be controlled by placing a guardrail at the location of the detector, but this will not correct the problem. While the hunting can be controlled, the variation due to wheel wear cannot be corrected.

For a revenue service application, shielding and cable protection are required to protect sensitive components. Figure 13 shows an alternative mounting with shields to protect sensors and cables. Several of this style mounting were tested as part of the prototype system.
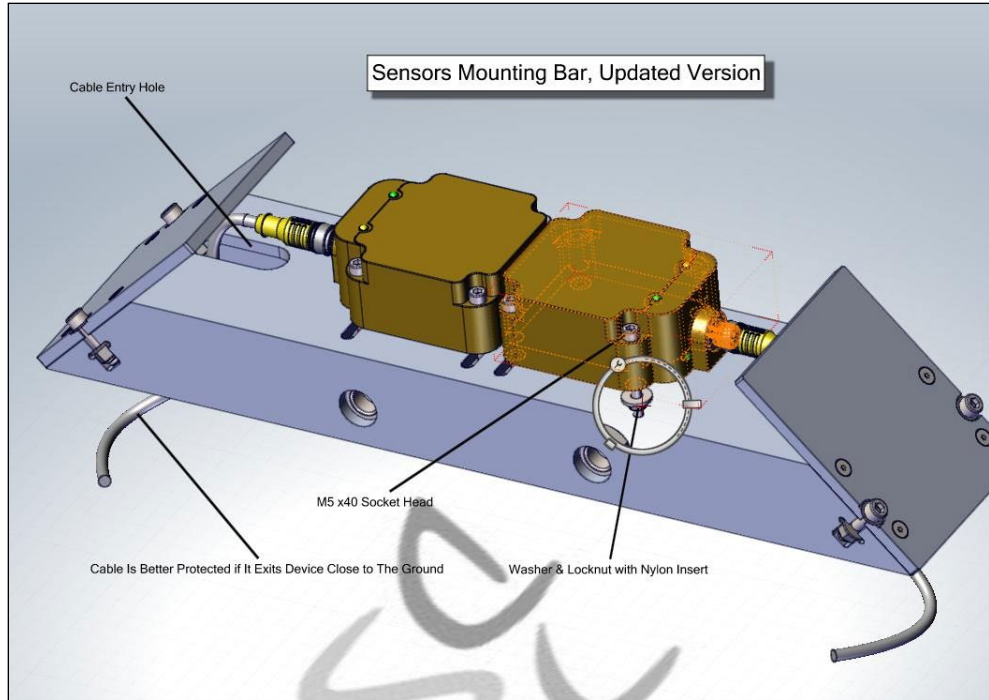
Figure 13. Service-ready Sensor Mounting Bracket with Shields

4. Installation

TTCI purchased the broken rim detector hardware on behalf of FRA and installed it at the Facility for Accelerated Service Testing (FAST) on the High Tonnage Loop (HTL) at the TTC. Figure 14 shows the prototype system. This system can sense wheels on both rails, but is only half as long as would be required to sense an entire wheel. This system provides enough to determine the feasibility of the concept.

Figure 14. Broken Rim Detector System Installed at the TTC

5. Testing

5.1 Sensor Reliability

Placing the broken rim detector at FAST on the HTL at TTC provides several unique advantages for cracked wheel testing. The HTL is the nightly service track for the FAST train. The train at FAST loops the 2.7-mile HTL every 4 minutes. This captive train provides an opportunity to sense the same population of wheels repeatedly. With this train, operating in a realistic service environment, statistically significant measures can be drawn that are not possible with the single pass of a revenue service train.

DII first determined signal reliability and variability of measurements during normal FAST train operation. Signal reliability was confirmed by comparing the number of wheel detections on the magnetic sensors to the counts from a digital wheel position sensor nearby. The magnetic sensors sensed 100 percent of the train wheels that passed the system at FAST. Perfect signal reliability is required of the sensors used in this application.

From the same measurements, DII generated statistics for signal length (amplitude). Table 1 shows the amplitude measurement statistics for a single pass of the train at FAST.

Table 1. Signal Amplitude Statistics for a Single Pass of the Train at FAST

Events	Maximum Amplitude	Minimum Amplitude	Average Amplitude
454	296	98	222

Table 2 gives the distribution results from this event, and Figure 15 shows the results graphically.

Table 2. Distribution of Amplitude Events for a Single Pass of the Train at FAST

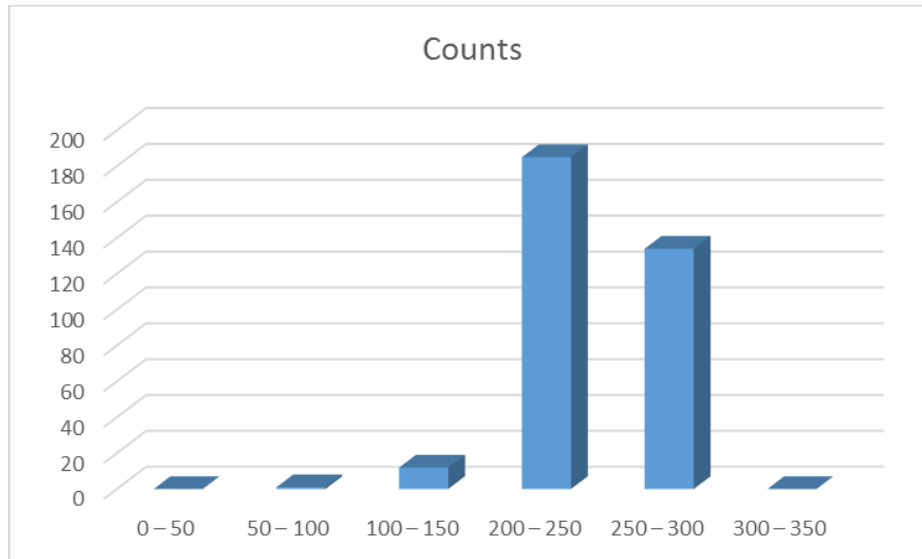| From–To	Counts
0–50	0
50–100	1
100–150	12
200–250	185
250–300	134
300–350	0

**Figure 15. Graph of Magnetic Sensor Amplitude Events for a Single Pass
of the Train at FAST**

From this analysis, DII determined that the sensors have suitable reliability, but that there is substantial variability in the average reading even for known good wheels. DII surmised that the readings must be normalized so that the average event per wheel is consistent for known good wheels. The deviation from sensor to sensor must be consistent for known good wheels if a deviation due to a wheel defect is to be detected. If the signals cannot be adequately normalized, then the system will not be able to detect anomalies due to missing material. Section 5.2 describes an adaptive routine to normalize the signals.

5.2 Calibration

The magnitude of the signal from the magnetic sensor depends on the distance between the sensor and the wheel. Several factors influence this distance. First is the amount of wheel tread overhanging the rail. The lateral position of the wheelset on the rail and width of the wheel tread will affect the distance to the sensor and thus the magnitude of the signal. Also, the position of each sensor relative to the railhead will influence the measurement. Both the side to side distance from the railhead and up and down position from top of rail will affect the straight-line distance to the rim. Finally, worn hollow wheel treads will also affect the result. Wheels with a hollow tread place the rim closer to the sensor than a freshly profiled wheel, which Figure 12 illustrates. The calibration procedure must distinguish the sensor position variations from the wheel geometry measurement in an objective way.

Figure 16 shows the signal from each of 12 sensors as a single wheel passes them sequentially.
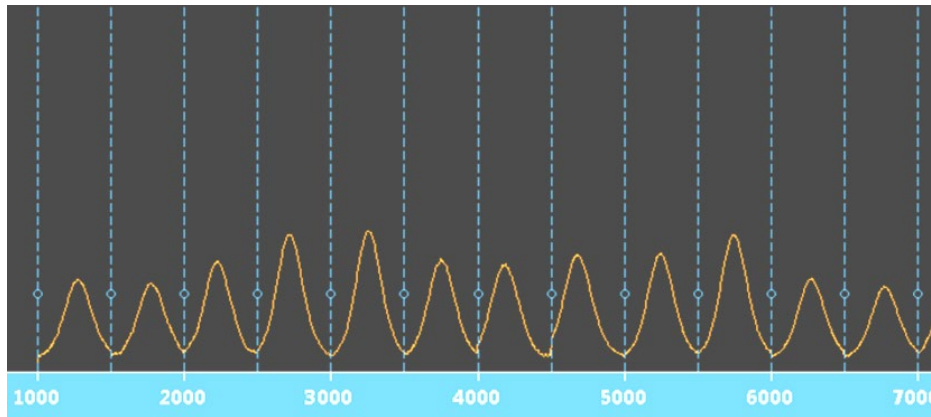
**Figure 16. Amplitude Readings from a Single Wheel
Passing a Magnetic Sensor on One Rail**

The relative magnitudes of the 12 signal amplitudes are similar for every wheel that passes. Sensors 1, 2, 7, 11, and 12 are consistently smaller. This means the sensors at these locations are installed lower or further away than the others. Figure 17 shows this on a three-dimensional bar chart. In this figure, there are 8 wheels passing 12 sensors.
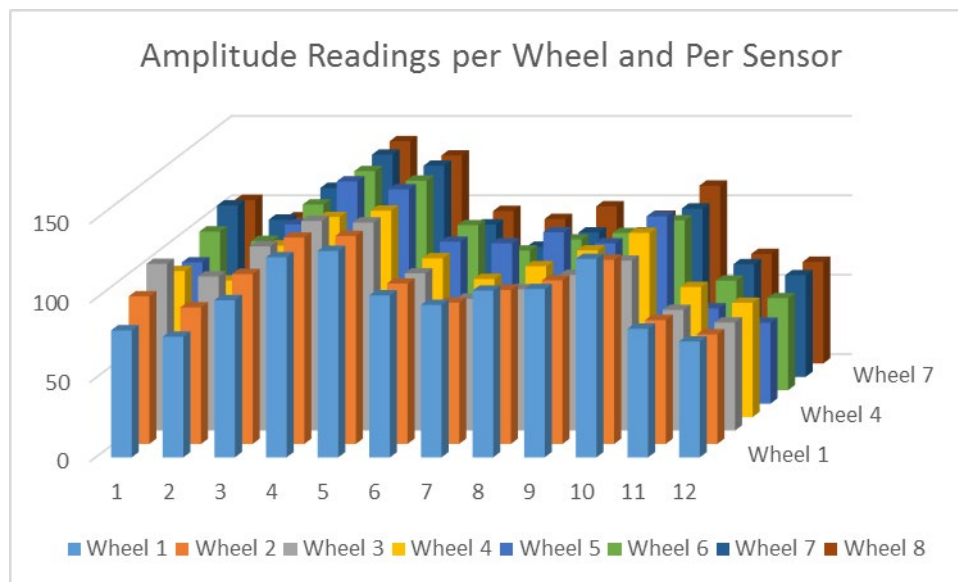

**Figure 17. Amplitude Readings Showing the Stronger
Dependency on Sensor Location than on Wheel**

The bars from front to back (i.e., relating to a given sensor) are more uniform than the bars from right to left (i.e., relating to a given wheel). This is favorable, because it means that the readings can be normalized on a per sensor basis. Readings that are normalized on a per sensor basis will emphasize the variation due to wheels only, which is what is required. Since the signal deviation from wheel to wheel is relatively consistent, this deviation can be used from mean as the calibration coefficient to eliminate the differences due to sensor positioning. The deviation is applied on a per axle basis. This is reasonable because the sum of readings across paired sensors is consistent for any pair of sensors. As the wheelset hunts move laterally, the left signal generally decreases in proportion to the increase in signal on the right side, so the sum of the

16

amplitudes on both wheels of an axle remains consistent. Once this calibration coefficient is applied to the data, the amplitudes per wheel are apparent, as shown in Figure 18.
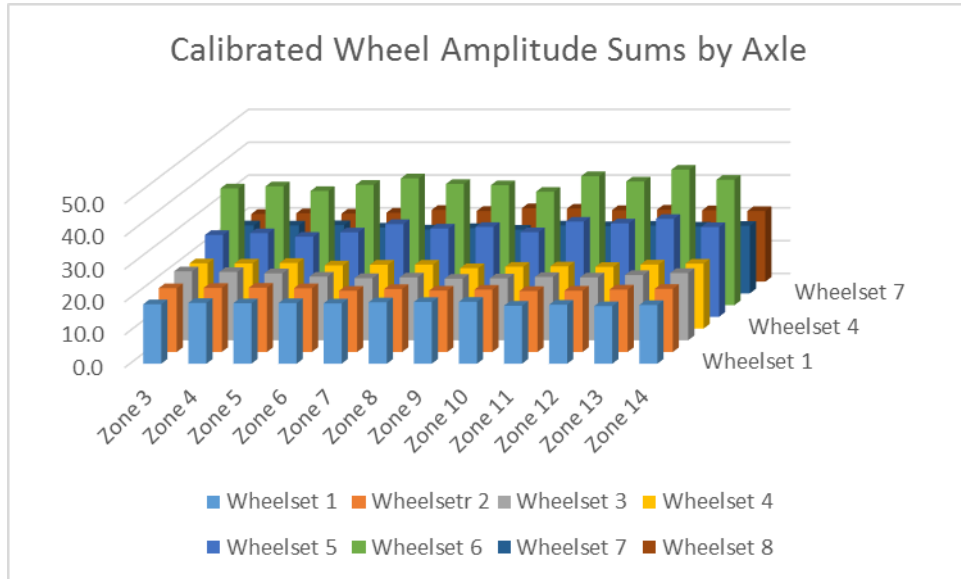

**Figure 18. Normalized Amplitude Readings, Normalized Using
Average Wheel Deviation per Axle**

For this 37-mph test, the average deviation per axle is 5 percent. When converted to a distance value, this corresponds to 0.06 inches (1.5 mm) deviation. This 0.06 inch (1.5 mm) represents the average difference in position of the rim segments over the sensors at this speed.

One would expect the normalized amplitudes to be consistent from sensor to sensor for an axle with two good wheels. This is the case for the first four wheelsets, which are the locomotive wheels. The following four wheelsets are from the test car and show greater average deviation. For axles 5 and 6, the deviation is about four times higher than on the other wheels. Section 6 explains the significance of these two wheels.

6. Results

TTCI produced a test wheel according to DII specification. The test wheel has three evenly spaced notches around the rim. Each one has a different depth. One is 0.25 inches (6.4 mm) deep, one is 0.50 inches (12.7 mm) deep, and one is 0.75 inch (19 mm) deep. All are 2 inches (50.8 mm) wide. Figure 19 shows the 0.75 inch (19 mm) deep notch. The mating wheel on the axle has no notches.

Figure 19. 0.75-inch Deep Rim Notch on the Test Wheel

TTCI installed this wheelset on a test car and operated it on the broken rim detector. This wheel was located at axle 5 on the train during the testing shown in Figure 18. The deviation between sensors for wheel 5 after correction suggests that the notched wheel can be detected. However, observe that the deviation for wheel 6 after correction is greater than the deviation for wheel 5. Wheel 6 has a continuous rim and should show lower deviation than wheel 5. Some underlying factor is more significant than the notch. TTCI and DII determined that this factor is hollow worn tread on wheel 6. The kinematics of the hollow tread create a nonlinearity in the rim elevation as the wheel displaces laterally. This nonlinearity in wheel position relative to the sensor is purely a function of wheel and rail geometry and cannot be corrected by the sensor deviation factor. The result is that the detector cannot be calibrated to detect wheels with broken tread before alarming on wheels with hollow worn tread.

This test was repeated with the notch lengths increased to 4 inches (101.6 mm) and the result was the same. The broken rim detector with magnetic sensors was still more sensitive to the worn rim than to the notched rim. TTCI and DII considered adding a guard rail to the detector to keep the wheels positioned laterally during sensing, but this was considered unnecessary as described in Section 6.1.

6.1 Analysis

Figure 20 shows the test wheel with the 0.75-inch (19 mm) slot perfectly aligned over one of the sensors.

18

Figure 20. Test Wheel Notch Aligned on One of the Magnetic Sensors

Unless the wheel was centered completely on the sensor, the reading was the same as if there were no slot. This ultimately becomes the limiting factor in using magnetic sensors for detecting missing material. Testing revealed that unless the void from missing material is larger than the sensing area of the magnetic sensor, then the sensor will detect the existing material and ignore the void. For in-service defects, the sensors must be much smaller than the ones selected for this testing. Smaller sensors could be used, but they would have to be mounted closer to the wheel, which creates clearance issues. This, along with the greater number of sensors required to sense the entire wheel makes such a system impractical.

The fundamental difference between ultrasonic sensors and magnetic sensors is that the ultrasonic sensors measure distance along line of sight, whereas the magnetic sensors detect presence of material. This creates a shortcoming for the magnetic sensors. The ultrasonic sensors measure distance to the edge of a body by sensing time of flight for the ultrasonic wave reflection. The measurement is focused on a small area in a straight line. If there is a void, it shows up as an aberration in the distance measurement. Magnetic sensors infer distance by measuring the strength of the magnetic field near the sensor. This measurement is spread out over the extent of the magnetic field. The closer the target is to the sensor, the more the magnetic field is deformed. However, magnetic sensors are less sensitive to surface geometry and more sensitive to average distance. If there is a void of material, the sensor still responds to the material closest to the void. This results in a "false" distance reading based on the average distance around the void unless the void is so large that the magnetic field is not altered at all. The geometry of many cracked rims is subtler than the notch in the calibration wheel, so the chances of detecting a service flaw with the magnetic sensors is extremely low.

7. Conclusion

From February to April 2014, TTCI researched new and emerging automated cracked wheel detectors under joint sponsorship of AAR and FRA. As part of this work, TTCI tested a concept called a broken rim detector from DII of Hackensack, NJ. The broken rim detector uses proximity sensors to detect the presence of rim material overhanging the field side of the rail. It is intended to find broken rims where a substantial chunk of material is missing. The concept was tested with both ultrasonic and magnetic sensors. The ultrasonic sensors were not suitable for the railroad environment. The device with magnetic sensors was determined to be insensitive to cracks typical of those that develop in service. It was shown to be more sensitive to tread wear than to a 0.75-inch deep by 4-inch long gouge on the corner of the wheel rim. TTCI determined that magnetic sensors are not practical for broken rim detection, because of the shortcomings of the magnetic sensors.

Abbreviations and Acronyms

ACRONYMS	EXPLANATION
AAR	Association of American Railroads
DII	Diesel Intellect International, Inc.
FAST	Facility for Accelerated Service Testing
FRA	Federal Railroad Administration
HTL	High Tonnage Loop
TTC	Transportation Technology Center (the site)
TTCI	Transportation Technology Center, Inc. (the company)